Modifying Adhesion of Linear Low-Density Polyethylene to Polypropylene by Blending with a Homogeneous Ethylene Copolymer

B. C. Poon,[1] S. P. Chum,[2] A. Hiltner,[1] E. Baer[1]

[1]*Department of Macromolecular Science and Engineering, and Center for Applied Polymer Research, Case Western Reserve University, Cleveland, Ohio 44106-7202*
[2]*Polyolefins and Elastomers R&D, The Dow Chemical Company, Freeport, Texas 77541*

Received 25 August 2003; accepted 29 September 2003

ABSTRACT: Adhesion of a Ziegler–Natta catalyzed ethylene copolymer (ZNPE) to polypropylene (PP) was studied by measuring the delamination toughness *G* of coextruded microlayers by using the T-peel test. Low values of *G* compared to a homogeneous copolymer with approximately the same short chain branch (SCB) content were attributed to an amorphous interfacial layer of low molecular weight, highly branched ZNPE fractions. Blending ZNPE with a homogeneous metallocene catalyzed copolymer (mPE) increased *G*. In this regard, mPE with higher SCB content was more effective than mPE with slightly lower SCB content. The ZNPE interface was mimicked by microlayering ZNPE and ZNPE blends with polystyrene from which the ZNPE layers were easily separated without damage to the surface. Examination with atomic force microscopy revealed a soft coating about 8 nm thick on the surface of the ZNPE layer. Blending with mPE reduced or eliminated the amorphous interfacial layer. It was proposed that mPE increased miscibility of low molecular weight, highly branched fractions of ZNPE and prevented their segregation at the interface. After blending with mPE eliminated the interfacial layer, *G* increased to a value comparable to that of a homogeneous copolymer with about the same SCB content as ZNPE bulk chains. The increase in *G* was attributed to epitaxial crystallization of the ethylene copolymer in the absence of an amorphous interfacial layer. © 2004 Wiley Periodicals, Inc. J Appl Polym Sci 92: 109–115, 2004

Key words: polyethylene; polypropylene; blends; adhesion; ethylene copolymers

INTRODUCTION

Conventional copolymerization of ethylene and an α-olefin with a Ziegler–Natta catalyst results in a linear low-density polyethylene (LLDPE) with broad molecular weight distribution and heterogeneous short-chain branch distribution. Heterogeneity in LLDPE takes the form of concentration of branches on lower molecular weight molecules. Segregation of highly mobile low molecular weight chains to the surface is well-known. In LLDPE blown film, segregation takes the form of an amorphous surface layer.[1,2] Metallocene-catalyzed copolymers possess homogeneous comonomer distribution and narrower molecular weight distribution. Lacking a population of low molecular weight chains that differ in composition from bulk chains, blown film does not possess a surface layer that is different from the bulk.[3]

The existence of a surface layer enriched in low molecular weight, highly branched fractions accounts for the unexpectedly long time scale for development of melt adhesion strength in LLDPE blown films.[1] Low molecular weight chains rapidly resolve the weld line; however, they cannot create good adhesion. Bulk chains need to diffuse through the amorphous layer to develop cohesive strength. The strength of the self-adhesion bond is of practical importance to heat seal and hot tack performance of polymeric films.[4,5]

Qualitatively, the driving force for segregation has both entropic and enthalpic origins. The entropic reason for segregation is halving in the conformational freedom of polymer chains on the surface compared to chains in the bulk. However, the shorter the chain, the less freedom it has and, hence, the less entropy is lost if the chain is located on the surface. The enthalpic reason for segregation is the decrease in surface energy due to the interaction of chain ends. The enthalpic advantage for surface segregation is enhanced considerably by increasing the concentration of chain ends, for example, by decreasing molecular weight or increasing the number of branches.

Blends of polypropylene (PP) and LLDPE can synergistically combine high stiffness and high heat deflection temperature of PP with low temperature toughness and good heat seal of LLDPE.[6] The same driving force that segregates low molecular weight, highly branched fractions to the surface of LLDPE film

Correspondence to: A. Hiltner (pah6@cwru.edu).
Contract grant sponsor: The Dow Chemical Co.

Journal of Applied Polymer Science, Vol. 92, 109–115 (2004)

TABLE I
Materials

Material description	Designation	Octene content (mol %)	Density (kg m^{-3})	I_2 [g (10 min)$^{-1}$]	M_w (kg mol^{-1})	MWD
Isotactic polypropylene (PROFAX® 6723)	PP	—	—	0.8	—	—
Polystyrene (STYRON® 665)	PS	—	—	1.0	—	—
Ziegler–Natta polyethylene (DOWLEX® 2083)	ZNPE	2.4	925	2.0	98	3.5
Metallocene polyethylene	mPE92	2.8	916	1.0	125	2.0
Metallocene polyethylene	mPE90	4.7	902	1.2	144	2.1
Metallocene polyethylene	mPE89	7.4	890	1.5	133	2.1

also accounts for concentration of these fractions at the interface of LLDPE domains in melt blends with PP.[7] Although polyethylene and polypropylene are generally considered to be immiscible, calculations predict an interfacial layer with thickness of 4–5 nm,[8] or roughly twice the radius of gyration of the entanglement molecular weight (M_e),[7,9] which is more than the minimum effective segment length of one M_e.[10] Poor adhesion of LLDPE to PP in melt blends is attributed to an amorphous interfacial layer of low molecular weight LLDPE fractions with a thickness of approximately 10 nm. Blends of metallocene-catalyzed copolymers with PP do not possess the amorphous interfacial layer and better adhesion is achieved through entanglements of average molecular weight chains in conformity with the prediction.[7]

Interfacial properties are not easily examined in the dispersed domain morphology of conventional melt blends. The goal of the present study is to directly access the interface between LLDPE and PP by using microlayers. Coextruded microlayers consist of many alternating layers of two polymers.[11,12] With the appropriate choice of coextrusion parameters, the individual layer thickness is of the same dimension as the domain size in conventional melt blends. Thus, the microlayer can be thought of as a one-dimensional blend.

The continuous interface is easily accessible to characterization of interfacial structure, and interfacial adhesion can be measured by the straightforward peel method.[13] The possibility that the driving force for segregation of low molecular weight LLDPE fractions can be reduced or eliminated entirely by blending with a homogeneous copolymer of higher short chain branch content is also explored in this communication.

EXPERIMENTAL

The polymers used in the study are described in Table I. The isotactic PP was PROFAX™ 6723 from Basell (Wilmington, DE); the Ziegler–Natta catalyzed ethylene copolymer (ZNPE) was DOWLEX™ 2083 from Dow Chemical Co., and the polystyrene (PS) was STYRON™ 665 from Dow. Three experimental metallocene-catalyzed ethylene-octene copolymers (mPE) that differed in comonomer content were provided by Dow. The melt flow index was measured at 190°C with a load of 2.16 kg (I_2). Temperature rising elution fractionation (TREF) curves of the ethylene copolymers in Figure 1 compare the SCB distribution of heterogeneous ZNPE and homogeneous mPE92, mPE90, and mPE89.

Blends of ZNPE with up to 37 wt % mPE were prepared in a Haake twin-screw extruder with barrel temperature set at 200°C. Blends were pelletized and coextruded as microlayers with PP in a 50 : 50 volume ratio. Tapes 12 mm wide and 1.6 mm thick with 33 alternating layers of PP and ZNPE or a ZNPE blend were coextruded. The outer layers were ZNPE or ZNPE blends. The layer thickness was approximately 50 μm. Microlayers of ZNPE and ZNPE blends with PS were coextruded under similar conditions.

Delamination was carried out with a modified T-peel test (ASTM D1876).[13] Strips 6.4 mm wide and 8 cm long were cut from the center of the tape and

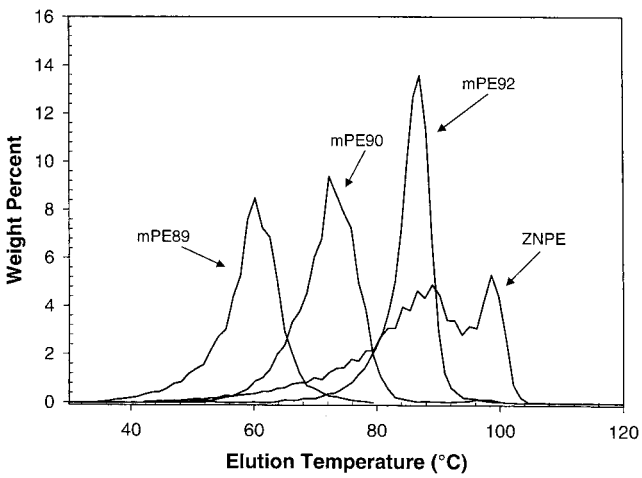

Figure 1 TREF curves of ethylene copolymers. Data provided by The Dow Chemical Co.

notched by pushing a fresh razor blade into the midplane of the tape. The notch was examined with an optical microscope to ensure that the crack started along a single interface. Specimens were peeled at ambient temperature at a rate of 1 mm min^{-1} in an Instron Model 1122. At least two specimens of each composition were tested.

Microlayers were microtomed at −45°C through the thickness of the tape and normal to the extrusion direction to expose a cross section of the layer interface. The microtomed surface was etched for 30 min by using a 2 : 1 vol : vol solution of sulfuric acid : orthophosphoric acid with 0.7 wt % potassium permanganate.[14] The etched surface was imaged in a Digital Instruments Nanoscope IIIa atomic force microscope (AFM) by using medium tapping with a set-point ratio (A/A_0) of 0.5 to 0.6 and a free oscillating tip amplitude of 36 nm. Height and phase images were recorded simultaneously.

Attempts to cryogenically separate the layers, to observe the layer surfaces, resulted in damage to the surfaces even for compositions with the poorest adhesion. The interface of ZNPE and ZNPE layers was mimicked by microlayering ZNPE and ZNPE blends with PS under identical processing conditions. The PS microlayers separated easily at liquid nitrogen temperature without damage to the surfaces. Surfaces of ZNPE and ZNPE blend layers were imaged by AFM. Imaging was performed under progressively harder tapping conditions by decreasing the set-point ratio (A/A_0) from 0.90 (light tapping) to 0.77 (harder tapping) with constant free oscillating tip amplitude of 36 nm.[3] Sometimes the ZNPE surface was washed with ethanol before imaging. The tip penetration depth was determined by the force-probe method. The lateral position of the tip was fixed and the amplitude of the oscillating cantilever was measured as a function of the tip-to-specimen distance.[3]

RESULTS AND DISCUSSION

Effect of chain heterogeneity on the interface with PP

The T-peel test is the most convenient method for comparing the effect of interfacial variables on adhesive strength of two flexible polymers.[15] However, peel tests do not supply absolute material data. Recognizing the limitations of the test, the testing conditions and specimen dimensions were maintained constant throughout the study. A typical load versus displacement peel curve consisted of an initial region where the load increased because of bending of the beam arms into the T-peel configuration followed by a steady-state region of crack propagation at constant load. In all cases, the crack propagated along the interface between a PP layer and a ZNPE layer as indicated by ATR-FTIR analysis of matching peel surfaces. This method probed to a depth of approximately 1 μm and showed only characteristic bands of ZNPE on one surface and only characteristic bands of PP on the matching surface. Crack propagation at constant peel force F allowed calculation of delamination toughness G from the relationship $G = 2F/w$, where w is the specimen width. For ZNPE, G was 140 J m^{-2}, whereas for homogeneous mPE92 with about the same SCB content as ZNPE, G was three times higher at 430 J m^{-2}.

Relatively poor adhesion of ZNPE to PP was attributed to segregation of low molecular weight, highly branched fractions of ZNPE to the interface during coextrusion.[7] Although these chains can interdiffuse with PP, their molecular weight is too low to produce effective entanglements. After solidification, the amorphous interfacial layer does not impart good adhesion to PP. Probing for an interfacial layer of composition different from the bulk required exposing the surface of the ZNPE layer. The interfacial layer should remain as a coating on the surface of the ZNPE layer where it could be detected by AFM. Because even the poorly adhering ZNPE layer could not be cryogenically separated from PP without causing some damage to the ZNPE surface, ZNPE and ZNPE blends were microlayered with PS. The same thermodynamic forces that drove low molecular weight fractions to the interface with PP also drove them to the PS interface. The ZNPE and PS layers easily separated cryogenically without damage to the layer surfaces.

Figure 2 depicts AFM phase images of the exposed ZNPE surface. The images were obtained with progressively harder tapping conditions. In phase images, soft amorphous material appears dark and hard crystalline material appears bright. Figure 2(a) shows that the ZNPE surface was covered with soft material. Numerous ridges revealed the contour of underlying crystalline lamellae. Occasional bright specks were segments of lamellar crystals that penetrated the soft surface coating. By tapping harder, the AFM tip penetrated the soft coating to reveal more of the underlying lamellar morphology [Fig. 2(b)]. Only the hardest tapping fully revealed the lamellar morphology in a section of a banded spherulite [Fig. 2(c)].

If the soft coating were composed of low molecular weight, amorphous fractions that had segregated to the interface, it should be possible to remove the coating by washing with a solvent. Figure 3 compares AFM phase images of the ZNPE surface before and after washing with ethanol. The images were obtained by using identical light tapping conditions with free oscillation amplitude of 36 nm and set-point ratio of 0.90. Lamellae were not visible on the unwashed surface [Fig. 3(a)]. In contrast, densely packed lamellae from a section of a banded spherulite were easily resolved on the washed surface by light tapping [Fig.

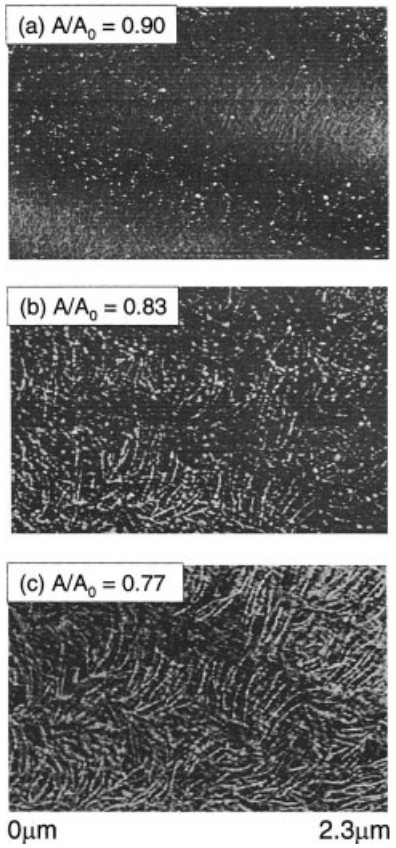

Figure 2 AFM phase images showing the layer surface of ZNPE under progressively harder tapping conditions with A_0 = 36 nm and A/A_0 as indicated.

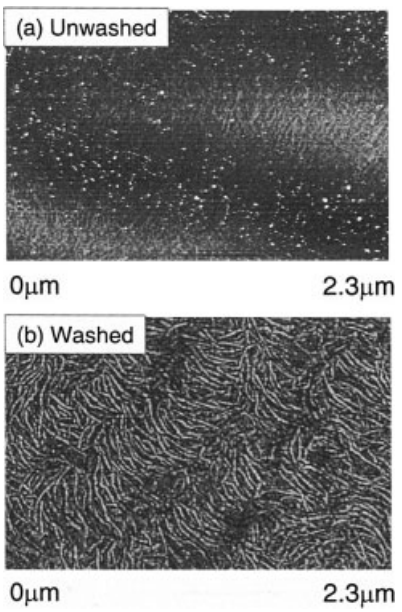

Figure 3 AFM phase images showing the layer surface of ZNPE with A_0 = 36 nm and A/A_0 = 0.90: (a) before ethanol wash; (b) after ethanol wash.

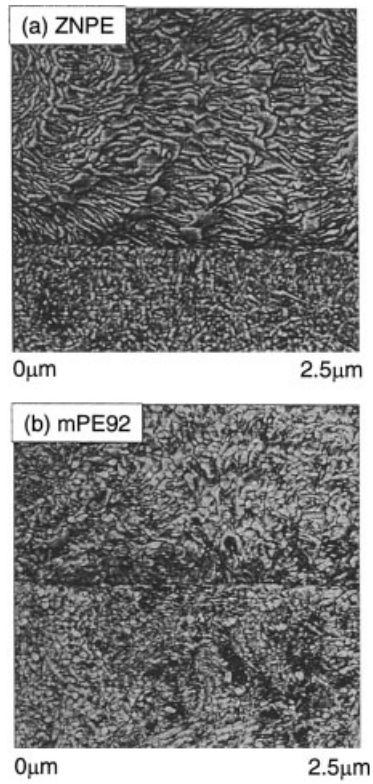

Figure 4 AFM phase images of microlayer cross sections showing the interface between an ethylene copolymer layer (upper layer) and a PP layer (lower layer): (a) ZNPE; (b) mPE92.

3(b)], demonstrating that the amorphous coating was removed.

The detrimental effect of the amorphous interfacial layer for adhesion to PP was evident from the difference, by a factor of 3, between G of ZNPE and G of homogeneous mPE92, which had about the same SCB content and molecular weight as the bulk chains of ZNPE. The effect of the amorphous layer on interaction between ZNPE and PP was probed by imaging cross sections of the interface with AFM. The interface in Figure 4(a) between ZNPE (upper layer) and PP (lower layer) was sharp and straight. The amorphous interfacial layer was too thin to be visible in the AFM image. The ZNPE side showed part of a spherulite that had nucleated in the bulk and had grown toward the interface until it impinged on the crystallized PP layer. There was no evidence of specific interactions between ZNPE and PP, such as epitaxial crystallization of ZNPE on the PP layer. The amorphous interfacial layer effectively prevented such interactions.

In contrast, the interface of mPE92 with PP contained numerous small lamellae that were mostly aligned parallel to the interface, although sometimes they were arranged at an angle of about 40° [Fig. 4(b)]. The aligned lamellae separated the PP layer at the bottom of the image from the PE spherulite at the top

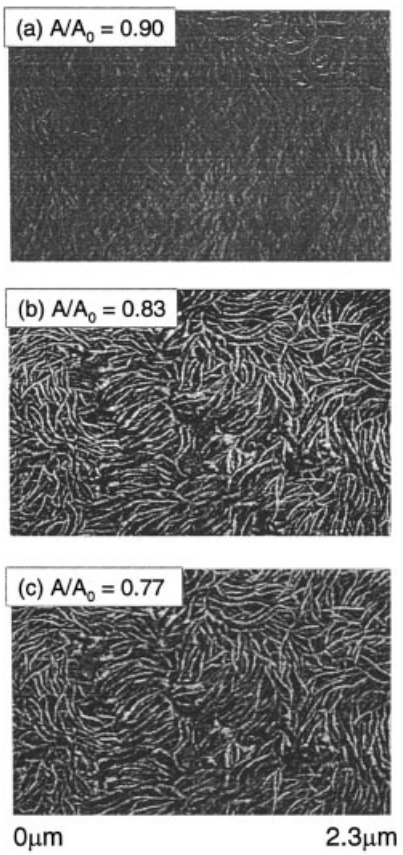

Figure 5 AFM phase images showing the layer surface of ZNPE blended with 25% mPE90 under progressively harder tapping conditions with A_0 = 36 nm and A/A_0 as indicated.

of the image. Epitaxial crystallization of high-density polyethylene on PP is well-known[16] and is known to enhance adhesion of polyethylene to PP.[17,18] Higher delamination toughness of mPE92 with the same SCB content as ZNPE was attributed to epitaxial crystallization of mPE92 in the absence of an amorphous interfacial layer.

Effect of blending ZNPE with mPE

Blending only 5% mPE89 with ZNPE increased G from 140 to 580 J m^{-2}, which was very close to the value for mPE92. Blending 5% mPE90, with lower SCB content than mPE89, was not as effective and increased G to only 220 J m^{-2}. Addition of 25% mPE90 was required to increase G to 630 J m^{-2}, a level comparable to that achieved with only 5% mPE89.

The increase in delamination toughness obtained by blending mPE with ZNPE was attributed to reduction or elimination of the amorphous interfacial layer. Figure 5 shows a layer surface of ZNPE blended with 25% mPE90 imaged by AFM with the same progressively harder tapping conditions used in Figure 2. The lightest tapping showed the surface topography with some bright lamellar segments [Fig. 5(a)]. Only slightly harder tapping clearly revealed the lamellar texture of a spherulite [Fig. 5(b)]. Comparison with Figure 2(b) demonstrated that this tapping condition was not hard enough to reveal lamellae on the ZNPE surface. The difference meant that blending 25% mPE90 with ZNPE reduced the thickness of the amorphous coating.

Increasing the mPE90 content to 37% eliminated the amorphous coating (Fig. 6). Even the lightest tapping conditions revealed lamellae that were part of a banded spherulite [Fig. 6(a)]. Slightly harder tapping only marginally improved the resolution of the lamellar morphology [Fig. 6(b)].

Although a blend of 25% mPE90 increased G to 630 J/m^2, only 5% mPE89 was required to achieve virtually the same increase in G to 580 J m^{-2}. Figure 7 shows the layer surface of ZNPE with 5% mPE89 imaged with the same sequence of progressively harder tapping conditions that was used to image the blend with 25% mPE90 in Figure 5. Comparison of Figures 7 and 5 shows that 5% mPE89 had virtually the same effect as 25% mPE90 in reducing the surface coating. Examination of exposed layer surfaces demonstrated that blending ZNPE with a homogeneous copolymer of higher SCB content resolved the amor-

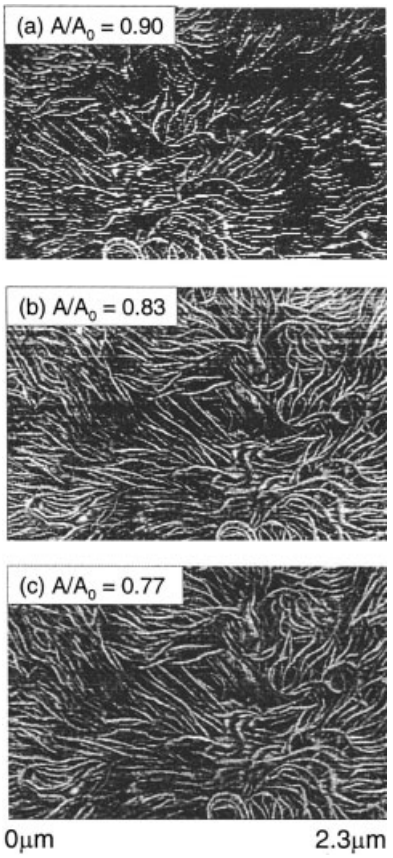

Figure 6 AFM phase images showing the layer surface of ZNPE blended with 37% mPE90 under progressively harder tapping conditions with A_0 = 36 nm and A/A_0 as indicated.

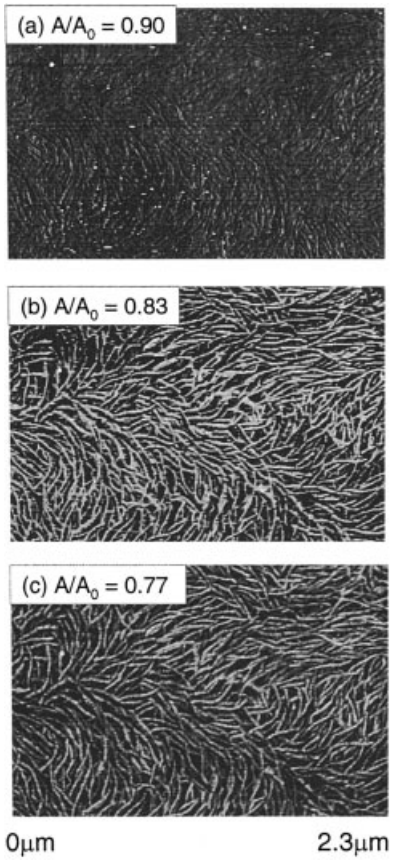

Figure 7 AFM phase images showing the layer surface of ZNPE blended with 5% mPE89 under progressively harder tapping conditions with A_0 = 36 nm and A/A_0 as indicated.

phous interfacial layer of ZNPE. In this regard, mPE89 with higher SCB content was more effective than mPE90.

Phase images provided only qualitative comparisons of different surfaces because identical tapping conditions gave deeper penetration on more compliant surfaces. To estimate the thickness of the amorphous coating, the penetration depth δ of the AFM tip was obtained by using the force-probe method.[3] Observation of constant δ over a range in set-point ratio was evidence that the measurements were meaningful. Reported values of δ were taken at a set-point ratio of 0.2, which was in the range of constant δ. Penetration depth is shown in Figure 8 as a function of free oscillation amplitude A_0, which is proportional to the maximum imposed force. As A_0 increased, the tip penetrated deeper into the coating. Initially, δ increased rapidly with A_0. The plateau at higher A_0 indicated a limit to the penetration depth. The ZNPE exhibited the highest penetration depth of approximately 15 nm. The maximum penetration depth decreased to 9 nm for the blend with 25% mPE90 and decreased further to 7 nm for the blend with 37% mPE90. These values were well within the reliable limit on penetration depth of soft surfaces, which appears to be in the range of 30–40 nm based on the maximum penetration depth measured under similar probe conditions for typical elastomers,[19] and for the amorphous layer on ZNPE blown film.[3] The tip penetration of the 37% mPE90 blend was attributed to bulk deformation only because a hard lamellar surface was imaged with the lightest tapping conditions (see Fig. 6). From the difference in penetration depth, the thickness of the ZNPE surface coating was estimated to be approximately 8 nm. This value is consistent with the estimated 10 nm thickness of the amorphous interfacial layer in melt blends of PP and LLDPE.[7]

Blends of ZNPE with mPE90 or mPE89 are miscible in the melt according to studies that establish the difference in comonomer content for melt miscibility as 8 mol % for this molecular weight range.[20] It appears that blending ZNPE with mPE of higher SCB content suppresses interfacial segregation of highly branched ZNPE fractions by enhancing their miscibility in the homogeneous melt and in the amorphous regions after solidification. The ZNPE bulk chains differ sufficiently in comonomer content from mPE89 chains that they do not cocrystallize.[21] Cooling in the microlayer process is slow enough for crystallization of ZNPE bulk chains to produce phase separation. The excluded phase consists of mPE89 chains together with highly branched ZNPE fractions. Considerable overlap between the main fractions of mPE89 and the highly branched tail of ZNPE in SCB distribution (Fig. 1) guarantees that the highly branched ZNPE fractions are miscible with the amorphous regions of mPE89 at all temperatures. It follows that blending a relatively small amount of mPE89 with ZNPE effectively eliminates segregation of the highly branched fractions to the interface.

With lower SCB content, mPE90 is less effective than mPE89 in promoting miscibility of highly branched ZNPE fractions in the melt and in prevent-

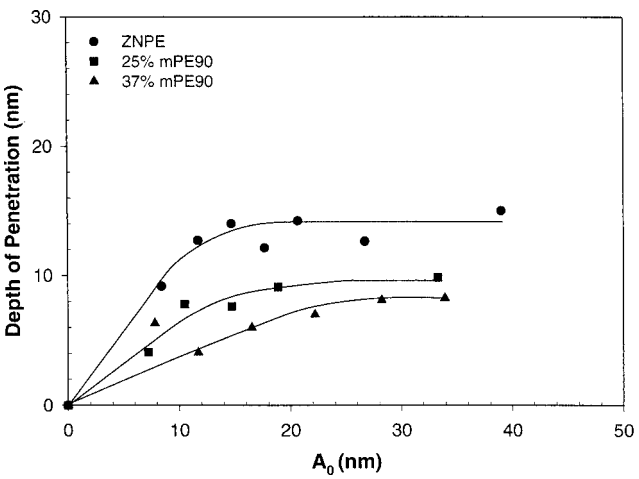

Figure 8 AFM penetration depth as a function of A_0.

ing their segregation at the interface. The main fractions of mPE90 do not overlap with the highly branched ZNPE fractions as well as the main fractions of mPE89 do in terms of SCB distribution. Consequently, the highly branched ZNPE fractions are less miscible with the amorphous regions after solidification. More mPE90 is required to prevent highly branched fractions from segregating at the interface. Indeed, a blend with 25% mPE90 is required to achieve the same interfacial characteristics as a blend with 5% mPE89.

A previous study demonstrated that bulk chains of ZNPE readily crystallize epitaxially on PP in the absence of an amorphous interfacial layer.[22] A similar effect can be achieved by blending. If ZNPE is blended with enough mPE89 or mPE90 to prevent segregation of low molecular fractions at the interface, ZNPE bulk chains are expected to epitaxially crystallize on PP during cooling. Epitaxial crystallization can be responsible for the increase in delamination toughness of ZNPE blends to a value comparable to the delamination toughness of a homogeneous copolymer with about the same SCB content as ZNPE bulk chains.

CONCLUSION

This study concerned the effect of chain heterogeneity on adhesion of a Ziegler–Natta catalyzed ethylene copolymer to PP. By using one-dimensional model blends prepared by microlayer coextrusion, it was possible to measure adhesion in terms of a delamination toughness G and to characterize the interfacial morphology. The study confirmed the existence of an amorphous interfacial layer of low molecular weight, highly branched fractions of ZNPE with a thickness of about 8 nm. The amorphous interfacial layer was detrimental to good adhesion. By preventing epitaxial crystallization of ZNPE bulk chains on PP, the amorphous interfacial layer accounted for lower G of ZNPE compared to a homogeneous ethylene copolymer of similar branch content as ZNPE bulk chains. Although the interfacial layer can be considered inherent to heterogeneous copolymers, interfacial segregation of highly branched fractions can be reduced or eliminated entirely by blending ZNPE with a homogeneous mPE of higher branch content. It is proposed that mPE increases miscibility of highly branched ZNPE fractions and prevents their segregation at the interface.

The technical assistance of Dr. L. Tau of The Dow Chemical Co. is gratefully acknowledged. Financial support for this research was provided by The Dow Chemical Co.

References

1. Qureshi, N. Z.; Stepanov, E. V.; Capaccio, G.; Hiltner, A.; Baer, E. Macromolecules 2001, 34, 1358.
2. Chang, A. C.; Chum, S. P.; Hiltner, A.; Baer, E. J Appl Polym Sci 2002, 86, 3625.
3. Qureshi, N. Z.; Rogunova, M.; Stepanov, E. V.; Capaccio, G.; Hiltner, A.; Baer, E. Macromolecules 2001, 34, 3007.
4. Mueller, C.; Capaccio, G.; Hiltner, A.; Baer, E. J Appl Polym Sci 1998, 70, 2021.
5. Halle, R. W.; Davis, D. S. Tappi J 1995, 78, 200.
6. Utracki, L. A.; Dumoulin, M. M. in Polypropylene Structure, Blends, and Composites; in Karger-Kocsis, J., Ed.; Copolymers and Blends; Chapman & Hall: New York, 1995; Vol 2, p. 50.
7. Chafin, K. A.; Bates, F. S.; Brant, P.; Brown, G. M. J Polym Sci, Part B: Polym Phys 2000, 38, 108.
8. Helfand, E.; Tagami, Y. J Chem Phys 1972, 56, 3592.
9. Fetters, L. J.; Lohse, D. J.; Richter, D.; Witten, T. A.; Zirkel, A. Macromolecules 1994, 27, 4639.
10. Creton, C.; Kramer, E. J.; Hadzioannou, G. Macromolecules 1991, 24, 1846.
11. Mueller, C. D.; Nazarenko, S.; Ebeling, T.; Schuman, T.; Hiltner, A.; Baer, E. Polym Eng Sci 1997, 37, 355.
12. Mueller, C.; Topolkaraev, V.; Soerens, D.; Hiltner, A.; Baer, E. J Appl Polym Sci 2000, 78, 816.
13. Ebeling, T.; Hiltner, A.; Baer, E. J Appl Polym Sci 1998, 68, 793.
14. Olley, R. H.; Bassett, D. C. Polymer 1982, 23, 1707.
15. Späth, T.; Plogmaker, D.; Keiter, S.; Petermann, J. J Mater Sci 1998, 33, 5739.
16. Lotz, B.; Wittmann, J. C.; Makromol Chem 1984, 185, 2043.
17. Chang, A. C.; Chum, S. P.; Hiltner, A.; Baer, E. Polymer 2002, 43, 6515.
18. Kestenbach, H.-J.; Loos, J.; Petermann, J. Polym Eng Sci 1998, 38, 478.
19. Bar, G.; Ganter, M.; Brandsch, R.; Delineau, L.; Wangbo, M.-H. Langmuir 2000, 16, 5702.
20. Stephens, C. H.; Hiltner, A.; Baer, E. Macromolecules 2003, 36, 2733.
21. Bensason, S.; Nazarenko, S.; Chum, S.; Hiltner, A.; Baer, E. Polymer 1997, 38, 3513.
22. Chang, A. C.; Tau, L.; Hiltner, A.; Baer, E. Polymer 2002, 43, 4923.